Spin Electronics

Terahertz-Frequency Signal Source Based on an Antiferromagnetic Tunnel Junction

Olga R. Sulymenko[1], Oleksandr V. Prokopenko[1], Vasyl S. Tyberkevych[2], and Andrei N. Slavin[2*]

[1] *Taras Shevchenko National University of Kyiv, Kyiv 01601, Ukraine*
[2] *Oakland University, Rochester, MI 48309, USA*
[*] *Fellow, IEEE*

Received 15 May 2018, revised 10 Jun 2018, accepted 11 Jun 2018, published 2 Jul 2018, current version 17 Jul 2018.

Abstract—We propose a novel type of terahertz-frequency (TF) signal source based on an antiferromagnetic tunnel junction (ATJ), where the generated ac signal is extracted through the variations of the tunneling anisotropic magnetoresistance (TAMR) of an ATJ. The signal source comprises a layered structure consisting of a current-driven platinum (Pt) layer and a layer of an antiferromagnet (AFM) separated by an MgO spacer from an additional Pt electrode. A dc electric current flowing in the first Pt layer due to the spin Hall effect creates a perpendicular spin current that, being injected in the AFM layer, tilts the magnetizations of the AFM sublattices and, therefore, causes TF rotation of these magnetizations in a large internal exchange magnetic field of the AFM. This rotation, through the TAMR effect, causes the TF variation of the total resistance of the layered structure. We evaluate the output power and efficiency of the above-described Pt/AFM/MgO/Pt TF signal source, and demonstrate that optimization of the source's geometrical parameters allows one to obtain the output power exceeding 1 μW at the frequency of 0.5 THz with the efficiency not smaller than 1%. Although the efficiency of the TAMR method of the TF signal extraction is reduced with the increase of the generation frequency, we believe that this method could be used for the generation of signals with frequencies of up to 10 THz due to its relative simplicity and convenience.

Index Terms—Spin electronics, terahertz frequency, signal source, antiferromagnet, tunnel junction, output power.

I. INTRODUCTION

Terahertz-frequency (**TF**) electromagnetic signals have a great potential for use in medical imaging and security applications, wireless communications and material characterization, bioelectronics and astronomy, etc. [Sirtori 2002, Kleiner 2007, Tonouchi 2007]. However, currently, there exist significant technical challenges in the development of compact, monochromatic, reliable, energy-efficient, and sufficiently high-output-power (the output power P_{ac} should be at least 1 μW) TF signal sources that delays the progress in the above-mentioned areas of the applied science and technology [Sirtori 2002, Kleiner 2007, Tonouchi 2007].

The existing methods of TF signal generation include various types of lasers [Köhler 2002, Hübers 2010, Nanni 2015], Josephson oscillators [Ozyuzer 2007], photodiodes [Tonouchi 2007], etc. However, all these methods require either complicated and bulky setups or cryogenic temperatures. Thus, it seems interesting and perspective to try to develop TF analogs of existing gigahertz-frequency (1–50 GHz) spintronic nano-oscillators [Kiselev 2003, Bonetti 2009, Slavin 2009, Prokopenko 2011, Demidov 2012, Chen 2016] based on ferromagnetic (**FM**) materials. Theoretical proposals for the development of such coherent and driven by a dc electric current spintronic TF signal generators, able to operate in the absence of a bias dc magnetic field, have been presented in Cheng [2016], Khymyn [2017], and Sulymenko [2017], and are based on the use of antiferromagnet (**AFM**) materials [Gomonay 2010, 2014, Jungwirth 2016].

One of the problems hindering the practical development of AFM-based TF signal generators is the problem of power extraction from such generators. In the first theoretical papers on this subject [Cheng 2016, Khymyn 2017], the inverse spin pumping into the Pt layer, based on the inverse spin Hall effect (**ISHE**) [Sinova 2015], has been proposed as a method of ac signal extraction from the device. The other power extraction mechanism, based on the registration of the magnetodipolar radiation from a current-driven *canted* AFM placed inside a high-Q resonator, has been analyzed in Sulymenko [2017]. Both these methods for TF signal extraction have some disadvantages.

For a generator utilizing ISHE, which is considered in detail in Khymyn [2017], the AFM material must be *bianisotopic* with a relatively weak perpendicular anisotropy (e.g., NiO). In such a spin-Hall oscillator (**SHO**), the ac signal created by the ISHE strongly decreases with the increase of the generation frequency, and it reaches a substantial power ($P_{ac} \sim 1$ μW) only in the range of relatively low frequencies, near the frequency of the in-plane antiferromagnetic resonance (approximately 100–300 GHz for a NiO SHO [Khymyn 2017]). In the case of a canted AFM-based SHO embedded in a high-Q dielectric resonator, the device could have a larger output power ($P_{ac} \sim$ 1–100 μW), but also has a larger size (∼10 μm) determined by the wavelength of the generated signal [Sulymenko 2017].

In this letter, we propose an alternative mechanism of the TF signal extraction from an AFM-based SHO, where the signal power is extracted through the ac variation of the tunneling anisotropic magne-

Corresponding author: Olga R. Sulymenko (e-mail: olgasulymenko@gmail.com).
Digital Object Identifier 10.1109/LMAG.2018.2852291

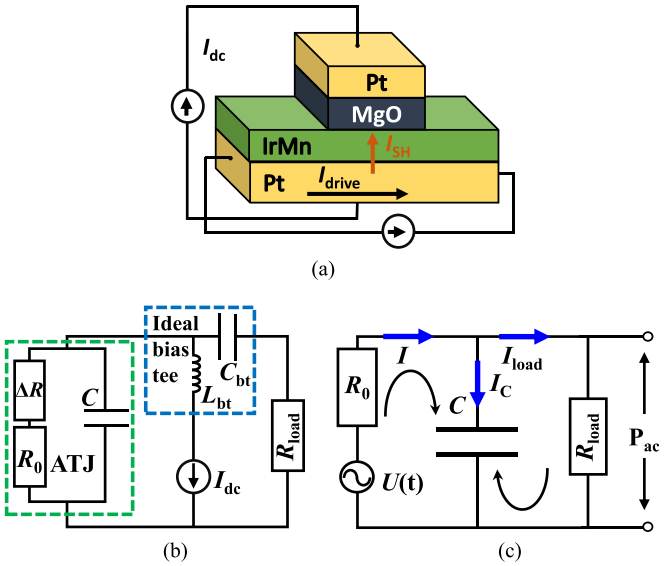

Fig. 1. (a) Schematics of an AFM-based Pt/IrMn/MgO/Pt source of TF signals. The driving dc current $I_{\rm drive}$ flowing in the bottom Pt layer of the AFM-based signal source generates the transverse spin current $I_{\rm SH}$ flowing into the AFM layer, which excites the TF rotation of magnetizations of the IrMn sublattices and, consequently, the TF variations of the junction resistance. When a bias dc current $I_{\rm dc}$ is simultaneously supplied to the junction, its action results in the generation of ac voltage $U(t)$ across the whole structure. (b) Equivalent electrical circuit of the considered ATJ loaded with a resistance $R_{\rm load}$. (c) Simplified equivalent circuit of the considered circuit at terahertz frequencies.

toresistance (**TAMR**) in an antiferromagnetic tunnel junction (**ATJ**), the electrical switching of which has been experimentally observed in recent works [Park 2011, Kriegner 2016, Wadley 2016]. In such an ATJ, the tunneling current across the MgO barrier was observed to strongly depend on the orientation of the AFM order parameter (Neel vector) in the used AFM material, and rotation of the AFM sublattices' magnetizations (and, therefore, the Neel vector) by approximately 90° resulted in the resistance change of 130% (giant TAMR) [Park 2011]. In that particular experiment, the AFM spins rotation was achieved by the exchange coupling of the AFM magnetization to the magnetization of an adjacent FM layer, and therefore, this approach in its direct form is not suitable for the development of TF devices because magnetic dynamics in FMs is too slow. However, as it will be shown in the following, the ATJs possessing a large value of TAMR could be promising for use in TF signal generation, if the junction is based on pure AFM materials and has no FM layers. The use of the TAMR effect for the TF signal extraction from an AFM-based signal generator removes the requirement of the *biaxial anisotropy* of the used AFM material, needed for the use of the ISHE signal extraction mechanism [Khymyn 2017], but brings a requirement that the used AFM material is conductive.

II. MODEL

We consider an antiferromagnetic SHO based on a Pt/$Ir_{0.2}Mn_{0.8}$/MgO/Pt tunnel junction structure shown in Fig. 1(a), where the driving dc current $I_{\rm drive}$ flowing in the Pt layer adjacent to the $Ir_{0.2}Mn_{0.8}$ (IrMn) layer forces a flow of a spin current $I_{\rm SH}$ into this layer due to the spin Hall effect [Sinova 2015]. This spin current excites the rotation of magnetizations of the IrMn AFM sublattices, which gives rise to the TF variations of the TAMR [Park 2011]. We assume that the junction resistance changes in time as $R(t) = R_0 + \Delta R \cos(\omega t)$, where $R_0 \equiv R_0(S,d) = {\rm RA}(0)\exp(\kappa d)/S$ is the equilibrium resistance of an ATJ, which depends on the thickness of the MgO barrier d, the effective junction's resistance–area product RA(0) (introduced for a "zero-thickness" MgO barrier), the intrinsic MgO barrier parameter κ [Hayakawa 2005, Yuasa 2007], and the junction cross-sectional area S; ΔR is the amplitude of the ac resistance variations in an ATJ, and $\omega = 2\pi f$ is the angular frequency of the resistance oscillations. Thus, the TAMR ratio η can be evaluated as $\eta = 2\Delta R/(R_0 - \Delta R)$, whereas ΔR can be calculated for a given η as $\Delta R = \eta R_0/(2+\eta)$. Note that the dependence of the resistance–area product of the ATJ on the MgO barrier thickness, $RA(d) = RA(0)\exp(\kappa d)$, was chosen to have the same form as for a conventional FM-based magnetic tunnel junction [Hayakawa 2005, Yuasa 2007].

While the driving current $I_{\rm drive}$ forces the excitation of the Neel vector rotation in the AFM IrMn layer and, consequently, creates resistance oscillations $R(t)$, the simultaneously supplied bias dc current $I_{\rm dc}$, traversing the junction cross section [see Fig. 1(a)], results in the generation of the ac voltage $U(t) = U_{\rm ac}\cos(\omega t) = I_{\rm dc}\Delta R\cos(\omega t)$ of the magnitude $U_{\rm ac} = I_{\rm dc}\Delta R$ across the whole structure. Taking into account that dc current $I_{\rm dc}$ flowing through an ATJ can be estimated as $I_{\rm dc} = U_{\rm dc}/R_0$, one can easily find the relation between the bias dc voltage $U_{\rm dc}$ and the magnitude of the generated ac voltage $U_{\rm ac}$: $U_{\rm ac} = U_{\rm dc}\eta/(2+\eta) = Ed\eta/(2+\eta)$. Here, we assume that dc voltage $U_{\rm dc}$ across the junction can be approximated by a simple linear dependence $U_{\rm dc} = Ed$, where an effective electric field E should be smaller than the breakdown field $E_{\rm max}$ for the MgO barrier ($E < E_{\rm max}$).

Hence, when such a dc-biased ATJ is connected through a bias tee to a load, having the resistance of $R_{\rm load}$, the ac voltage $U(t)$ generated in the ATJ excites an ac current in the load $I_{\rm load}(t)$, which allows one to extract the ac power $P_{\rm ac}$ of the generated signal from the load.

We consider an ATJ as an electric circuit consisting an ac voltage source [generating ac voltage $U(t)$] with the internal resistance R_0 shunted by a capacitor of the capacitance $C \approx \varepsilon\varepsilon_0 S/d$, where ε is the relative permittivity of the MgO layer, and ε_0 is the permittivity of a vacuum. In our model, we neglect the internal inductance of an ATJ, which can be estimated as $L \sim \mu_0 d \sim 3\times10^{-15}$ H. The corresponding impedance at 1 THz, $X_L = \omega L \sim 0.02\,\Omega$ is much smaller than all the other resistances in the considered circuit, and therefore, the ATJ inductance can be ignored. This equivalent circuit is connected through an ideal bias tee (having the inductance $L_{\rm bt}$ and capacitance $C_{\rm bt}$) to a resistive load of the resistance $R_{\rm load}$ (wave impedance of an external circuit) [see Fig. 1(b)].

The ideal bias tee has no influence on the generated ac signal. It just separates the dc and ac currents in the considered circuit, which allows one to exclude this bias tee from the analysis and consider a simplified equivalent ac signal circuit shown in Fig. 1(c). The complex amplitudes of the ac currents and ac voltages in this circuit are governed by Kirchhoff's laws: $I_C + I_{\rm load} = I$, $IR_0 + I_C/(i\omega C) = U_{\rm ac}$, $-I_C/(i\omega C) + I_{\rm load}R_{\rm load} = 0$, where I, I_C, and $I_{\rm load}$ are the complex amplitudes of ac currents flowing through the circuit branches with ac voltage source, the junction's capacitor, and the load, respectively, and $i = \sqrt{-1}$. The solution of these equations can be easily found as $I = I_{\rm ac}(\beta r - i)/q$, $I_C = I_{\rm ac}\beta r/q$, $I_{\rm load} = -iI_{\rm ac}/q$, where $I_{\rm ac} = U_{\rm ac}/R_0$, and $q \equiv q(\beta, r) = \beta r - i(r+1)$. We also introduced

two dimensionless parameters: $\beta = \omega R_0 C$, which characterizes time delay or phase properties of an ATJ, and resistance ratio $r = R_{\text{load}}/R_0$, which serves as ATJ's amplitude characteristic.

Using the formula for I_{load}, we found the following expressions for the ac power in the load:

$$P_{\text{ac}} = \frac{1}{2}|I_{\text{load}}|^2 R_{\text{load}} = \left(\frac{U_{\text{ac}}^2}{2R_{\text{load}}}\right)\frac{r^2}{(r+1)^2 + r^2\beta^2} \tag{1}$$

whereas the dc power provided to the ATJ P_{dc} can be evaluated as $P_{\text{dc}} = I_{\text{dc}}^2 R_0 = U_{\text{dc}}^2/R_0 = U_{\text{dc}}^2 r/R_{\text{load}}$. Then, the efficiency of the ac power extraction from an ATJ via the resistive load can be estimated as

$$\zeta = \frac{P_{\text{ac}}}{P_{\text{dc}}} = \frac{1}{2}\left(\frac{\eta}{2+\eta}\right)^2 \frac{r}{(r+1)^2 + r^2\beta^2}\,. \tag{2}$$

Here, in the expression for efficiency (2), we neglect the influence of the drive dc current I_{drive}, because in a typical situation when the SHO generates rather high output power (so $I_{\text{dc}} \gg I_{\text{drive}}$), the dc power used for the excitation of TAMR oscillations $P_{\text{drive}} = I_{\text{drive}}^2 R_{\text{Pt}}$ is substantially smaller than the bias dc power P_{dc} (R_{Pt} is the resistance of Pt layer). With an account of P_{drive}, the modified efficiency $\tilde{\zeta} = P_{\text{ac}}/(P_{\text{dc}} + P_{\text{drive}})$ could be slightly less than ζ, $\tilde{\zeta} \approx 0.9\zeta$.

III. RESULTS AND DISCUSSION

Before discussing the numerical calculations describing the performance of the proposed ac signal source based on an ATJ, it is useful to perform a simple qualitative analysis of the obtained equations (1) and (2).

First, the presence of the term $\sim\beta^2 = (2\pi f R_0 C)^2$ in the denominators in (1) and (2) shows that both the output ac power P_{ac} and the efficiency ζ of the proposed signal source should decrease with the increase of the signal frequency f. Consequently, such ac sources can have satisfactory performance only in the low-frequency part of the terahertz frequency range, and only if a junction having relatively a low capacitance C and equilibrium resistance R_0 is used. Note, also, that $R_0 \sim S^{-1}$, whereas $C \sim S$, so in the chosen model, the parameter $\beta \sim R_0 C$ does not depend on the junction cross-sectional area S, and it can be varied only by choosing an appropriate value of the MgO barrier thickness d.

Second, the output ac power P_{ac} and the efficiency ζ of the signal source are greatly reduced when the equilibrium ATJ resistance R_0 is substantially larger or smaller than the load resistance R_{load}. Hence, the proposed source can have a sufficiently good performance only if the load and junction resistances are almost equal ($R_{\text{load}} \approx R_0$). Usually, the load resistance R_{load} is considered to be a fixed parameter, defined by an existing experimental setup, measuring technique, etc. Thus, to reach the optimal condition $R_{\text{load}} \approx R_0$, one can vary the cross-sectional area S of the junction and the thickness d of the MgO tunneling barrier.

Third, the efficiency of the generator $\zeta \sim \eta^2/(2+\eta)^2$ increases with the increase of the TAMR ratio η, so the increase of the TAMR ratio η is clearly beneficial for the characteristics of the AFM signal source. Although in this letter we consider the TAMR ratio η as a given experimentally defined parameter, in practice an additional tuning of the signal source's performance can be achieved via the tuning of the η value by applying to ATJ a bias dc magnetic field, or by changing the temperature of the sample. However, the influence of the temperature on ζ and P_{ac} in an AFM-based SHO could be substantially nonlinear, similar to the behavior of FM-based magnetic tunnel junctions [Shang 1998, Prokopenko 2012].

In our calculations, we used the following typical experimental parameters of an ATJ [Park 2011]: equilibrium resistance $R_0 = 55.0\,\text{k}\Omega$, TAMR ratio $\eta = 1.3$, junction cross-sectional area $S = 1 \times 5\,\mu\text{m}^2$, and thickness of MgO barrier $d = 2.5$ nm. Assuming that for an ATJ the influence of the tunneling barrier thickness d on the junction resistance is similar to that for an FM-based junction, we estimated using Hayakawa [2005] and Yuasa [2007] the value of the intrinsic MgO barrier parameter $\kappa \approx 5.8\ \text{nm}^{-1}$. Then, using these parameters, we found the values of an effective resistance–area product $\text{RA}(0) \approx 0.14\,\Omega \cdot \mu\text{m}^2$ and the magnitude of the ac resistance $\Delta R \approx 21.7\ \text{k}\Omega$. Also, a relative permittivity ε of the MgO barrier was chosen to be $\varepsilon = 9.8$ [Raj 2010]; hence, the junction capacitance can be estimated as $C = \varepsilon\varepsilon_0 S/d = 1.7 \times 10^{-13}$ F. Since the breakdown electric field for an MgO thin film has a value of $E_{\text{max}} = 0.4 - 0.6$ V/nm [Raj 2010], for a stable regime of the ATJ operation we chose a smaller value of the applied electric field $E = 0.3$ V/nm, and considered the dc voltage applied to the junction as a function of the barrier thickness d: $U_{\text{dc}} \equiv U_{\text{dc}}(d) = Ed$. Finally, we assumed that the load resistance R_{load} has a standard value, that is, typical for microwave and terahertz electronics $R_{\text{load}} = 50\,\Omega$.

The output ac power P_{ac} and efficiency ζ, calculated from (1) and (2) for the signal source having typical experimental parameters presented above, demonstrate that both these characteristics are decreasing with the increase of the generated frequency f, and the absolute values of the power P_{ac} and the efficiency ζ are very small, even at sufficiently low frequencies ($P_{\text{ac}} \sim 10^{-5}\,\mu\text{W}$, $\zeta \sim 10^{-4}\%$ at $f \sim 0.1$ THz) due to the rather large junction resistance R_0 and capacitance C, which unfavorably affects the value of the parameter β ($\beta = \omega R_0 C \gg 1$) and causes a low input dc power $P_{\text{dc}} \sim 1/R_0$, as well as a poor resistance matching ($r = R_{\text{load}}/R_0 \ll 1$). All this means that ATJs with typical experimental parameters (for instance, similar to the ones used in Park [2011] and having rather large resistance R_0 and capacitance C) are not suitable for the development of effective TF signal sources.

It became clear from our analysis that the working characteristics of an ATJ-based TF signal source can be optimized by varying the cross-sectional area S and MgO barrier thickness d of the used ATJ. For instance, the ATJ equilibrium resistance R_0 depends on S and d as $R_0 \sim \exp(\kappa d)/S$, whereas the junction capacitance on $C \sim S/d$. By varying both these geometrical parameters of the junction, one can tune and optimize the performance of the proposed ac signal source. The results of these calculations are presented in Fig. 2.

As expected, an influence of the MgO barrier thickness d on the output ac power P_{ac} and efficiency ζ is very strong due to the exponential dependence of $\text{RA}(d)$, and therefore, the barrier thickness d should be considered as a main optimization parameter. It can be seen from Fig. 2(a) that P_{ac} and ζ are, generally, monotonically increased with the decrease of the MgO layer thickness d, and can reach their maximum values at rather small, but frequency-dependent, values of d (for instance, $d \approx 0.8$ nm at $f = 0.1$ THz), when the internal junction resistance R_0 becomes comparable to the load resistance R_{load}.

We emphasize that further decrease of d does not lead to the increase of P_{ac} and ζ. On the contrary, in an ATJ with a sufficiently thin MgO barrier ($d \leq 0.5$ nm), both these characteristics may be reduced due

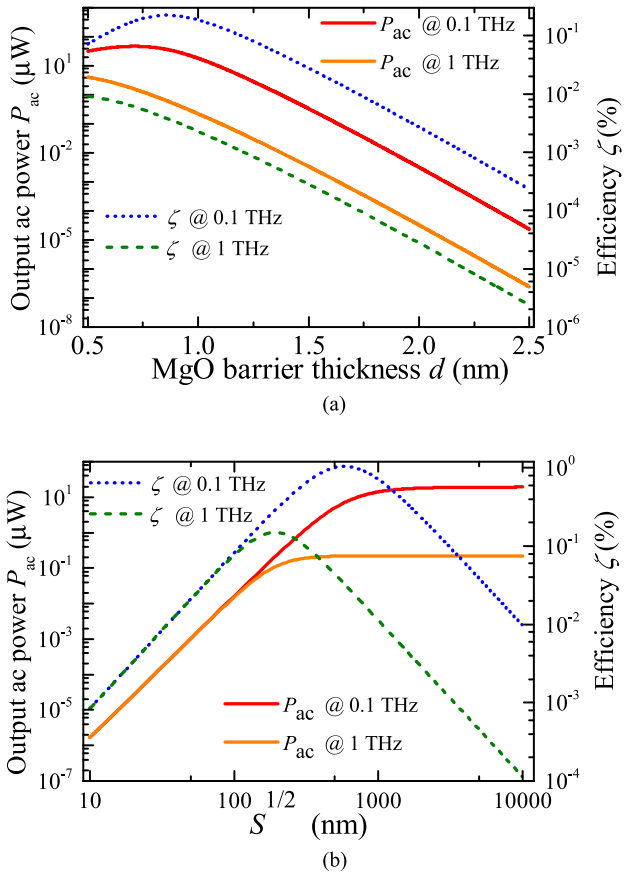

Fig. 2. Dependence of the output ac power P_{ac} (solid lines) and the energy conversion efficiency ζ (dashed lines) of the proposed TF signal source on (a) MgO barrier thickness d and (b) lateral size of the ATJ square-cross-section $a = \sqrt{S}$. Calculations were performed using (1) and (2) for an ATJ with typical experimental parameters (see Section III for details) operating at the frequencies $f = 0.1$ THz and $f = 1.0$ THz. In (b), the optimal thickness of the MgO barrier $d_{opt} = 1.0$ nm was used.

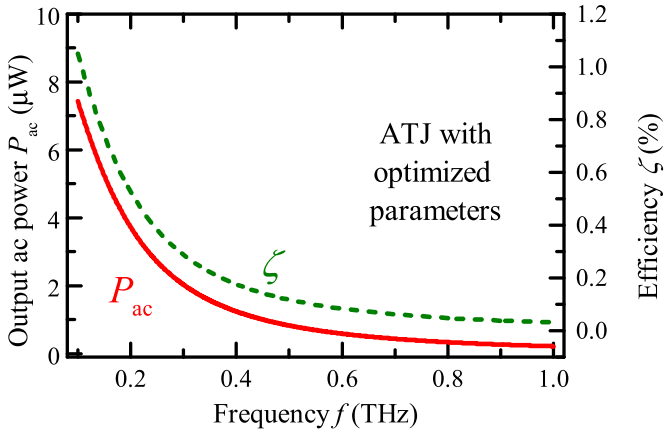

Fig. 3. Frequency dependence of the output ac power P_{ac} (solid line) and the energy conversion efficiency ζ (dashed line) of the proposed TF signal source calculated from (1) and (2), respectively, for an ATJ with optimized experimental parameters ($d_{opt} = 1.0$ nm, $a_{opt} = 600$ nm, see also Section III for details).

to the increase of the resistance mismatch and junction capacitance $C \sim 1/d$ and reduction of the applied dc voltage $U_{dc} = Ed$. Taking into account these results, in the following we consider an ATJ having *optimal* MgO barrier thickness of $d_{opt} = 1.0$ nm, which is quite a common value for the existing tunnel junctions [Hayakawa 2005, Yuasa 2007, Raj 2010].

An additional improvement of the ac signal source performance can be achieved by choosing the optimal lateral sizes of an ATJ. Considering, for simplicity, a square junction with a single effective lateral junction size $a = \sqrt{S}$, one can calculate from (1) and (2) the lateral size dependences of P_{ac} and ζ on a, as shown in Fig. 2(b). As one can see, the dependence $\zeta(a)$ (dotted blue line) has a clear maximum, the position of which shifts to smaller values of $a = \sqrt{S}$ with the increase of the signal frequency f. The position of this maximum corresponds to the optimal value of the second geometrical parameter of an ATJ, $a = \sqrt{S} = a_{opt}$. At $a < a_{opt}$, the performance of the signal source is hindered mainly due to the resistance mismatch effect, while at $a > a_{opt}$ the efficiency reduction is caused by the influence of the large junction capacitance.

Note, also, that the behavior of $P_{ac}(a)$ is quite different. For a small junction size, the output ac power P_{ac} dramatically increases with a (due to the decrease of R_0), but, then, at $a \approx a_{opt}$, the dependence $P_{ac}(a)$ becomes almost saturated (due to the influence of the junction's capacitance $C \sim a^2$).

The results presented in Fig. 2 show that optimization of the ATJ geometrical parameters allows one to achieve working characteristics of the ATJ-based TF signal sources that are sufficiently high for a number of practical applications. In particular, it follows from Fig. 2(b) that generators operated at higher frequencies should utilize smaller size ATJs (for instance, $a_{opt} \approx 600$ nm at $f = 0.1$ THz and $a_{opt} \approx 200$ nm at $f = 1.0$ THz).

The frequency dependences of the power P_{ac} and efficiency ζ for the ATJ-based signal source having optimal parameters $d_{opt} = 1.0$ nm, $a_{opt} = 600$ nm are shown in Fig. 3 by solid and dashed lines, respectively. The calculated curves demonstrated that the output power P_{ac}, on a standard load obtained from an optimized AFM-based SHO in the frequency range 0.1–1 THz, is comparable to, or may even exceed, the power extracted via ISHE [Khymyn 2017] and a magnetodipole emission mechanism [Sulymenko 2017], whereas the efficiency of the power extraction mechanism via the ac TAMR variations is about 1%. The generated power is rather large, about 100 nW or more, and the presence of TF radiation can be registered, e.g., by commercially available pyroelectric detectors working at room temperature. Also, this radiation emission could be maximized if the generating SHO is embedded into a TF transmission line or resonator, and the wave impedance matching conditions are fulfilled.

If a particular value of the generated frequency f is selected, then one can perform an optimization procedure presented above and achieve the values of P_{ac} and ζ, larger than the ones presented in Fig. 3 (improvement of P_{ac} is about 1–2 μW, ζ increases up to about 1.2%), for a source generating a quasi-monochromatic ac signal at a frequency f. Note, also, that a substantial advantage of the proposed generator with a signal extraction through the ac TAMR lies in the simplicity of its experimental realization at micro- and nanoscale. In addition to that, the decrease of the lateral sizes of a generating ATJ with the increase of its generation frequency could be useful for the development of sufficiently large-output-power microscale sources based on arrays of ATJs operating in the TF range.

ACKNOWLEDGMENT

This work was supported in part by the "President's of Ukraine" Grant F 78; in part by the Grant F 76 from the State Fund for Fundamental Research of Ukraine; in part by the Grant EFMA-1641989 and Grant ECCS-1708982 from the National Science Foundation of the USA; in part by the DARPA M3IC Grant under the Contract W911-17-C-0031; in part by Grant 16BF052–01 and Grant 18BF052–01M from the Taras Shevchenko National University of Kyiv; and in part by the Grant 7F from the National Academy of Sciences of Ukraine.

REFERENCES

Bonetti S, Muduli P, Mancoff F, Åkerman J (2009), "Spin torque oscillator frequency versus magnetic field angle: The prospect of operation beyond 65 GHz," *Appl. Phys. Lett.*, vol. 94, 102507, doi: 10.1063/1.3097238.

Chen T, Dumas R K, Eklund A, Muduli P K, Houshang A, Awad A A, Dürrenfeld P, Malm B G, Rusu A, Åkerman J (2016), "Spin-torque and spin-Hall nano-oscillators," *Proc. IEEE*, vol. 104, pp. 1919–1945, doi: 10.1109/JPROC.2016.2554518.

Cheng R, Xiao D, Brataas A (2016), "Terahertz antiferromagnetic spin Hall nano-oscillator," *Phys. Rev. Lett.*, vol. 116, 207603, doi: 10.1103/PhysRevLett.116.207603.

Demidov E V, Urazhdin S, Ulrichs H, Tiberkevich V, Slavin A, Baither B, Schmitz G, Demokritov S O (2012), "Magnetic nano-oscillator driven by pure spin-current," *Nature Mater.*, vol. 11, pp. 1028–1031, doi: 10.1038/nmat3459.

Gomonay H V, Loktev V M (2010), "Spin transfer and current-induced switching in antiferromagnets," *Phys. Rev. B*, vol. 81, 144427, doi: 10.1103/PhysRevB.81.144427.

Gomonay E V, Loktev V M (2014), "Spintronics of antiferromagnetic systems," *Low Temp. Phys.*, vol. 40, pp. 17–35, doi: 10.1063/1.4862467.

Hayakawa J, Ikeda S, Matsukura F, Takahashi H, Ohno H (2005), "Dependence of giant tunnel magnetoresistance of sputtered CoFeB/MgO/CoFeB magnetic tunnel junctions on MgO barrier thickness and annealing temperature," *Jpn. J. Appl. Phys.*, vol. 44, pp. 587–589, doi: 10.1143/JJAP.44.L587.

Hübers H-W (2010), "Terahertz technology: Towards THz integrated photonics," *Nature Photon.*, vol. 4, pp. 503–504, doi: 10.1038/nphoton.2010.169.

Jungwirth T, Marti X, Wadley P, Wunderlich J (2016), "Antiferromagnetic spintronics," *Nature Nanotechnol.*, vol. 11, pp. 231–241, doi: 10.1038/NNANO.2016.18.

Khymyn R, Lisenkov I, Tiberkevich V, Ivanov B A, Slavin A (2017), "Antiferromagnetic THz-frequency Josephson-like oscillator driven by spin current," *Sci. Rep.*, vol. 7, 43705, doi: 10.1038/srep43705.

Kiselev S I, Sankey J C, Krivorotov I N, Emley N C, Schoelkopf R J, Buhrman R A, Ralph D C (2003), "Microwave oscillations of a nanomagnet driven by a spin-polarized current," *Nature*, vol. 425, pp. 380–383, doi: 10.1038/nature01967.

Kleiner R (2007), "Filling the terahertz gap," *Science*, vol. 318, pp. 1254–1255, doi: 10.1126/science.1151373.

Köhler R, Tredicucci A, Beltram F, Beere H E, Linfield E H, Davies A G, Ritchie D A, Iotti R C, Rossi F (2002), "Terahertz semiconductor-heterostructure laser," *Nature*, vol. 417, pp. 156–159, doi: 10.1038/417156a.

Kriegner D, Výborný K, Olejník K, Reichlová H, Novák V, Marti X, Gazquez J, Saidl V, Němec P, Volobuev V V, Springholz G, Holý V, Jungwirth T (2016), "Multiple-stable anisotropic magnetoresistance memory in antiferromagnetic MnTe," *Nature Commun.*, vol. 7, 11623, doi: 10.1038/ncomms11623.

Nanni E A, Huang W R, Hong K-H, Ravi K, Fallahi A, Moriena G, Miller R J D, Kärtner F X (2015), "Terahertz-driven linear electron acceleration," *Nature Commun.*, vol. 6, 8486, doi: 10.1038/ncomms9486.

Ozyuzer L, Koshelev A E, Kurter C, Gopalsami N, Li Q, Tachiki M, Kadowaki K, Yamamoto T, Minami H, Yamaguchi H, Tachiki T, Gray K E, Kwok W-K, Welp U (2007), "Emission of coherent THz radiation from superconductors," *Science*, vol. 318, pp. 1291–1293, doi: 10.1126/science.1149802.

Park B G, Wunderlich J, Martí X, Holý V, Kurosaki Y, Yamada M, Yamamoto H, Nishide A, Hayakawa J, Takahashi H, Shick A B, Jungwirth T (2011), "A spin-valve-like magnetoresistance of an antiferromagnet-based tunnel junction," *Nature Mater.*, vol. 10, pp. 347–351, doi: 10.1038/nmat2983.

Prokopenko O, Bankowski E, Meitzler T, Tiberkevich V, Slavin A (2011), "Spin-torque nano-oscillator as a microwave signal source," *IEEE Magn. Lett.*, vol. 2, 3000104, doi: 10.1109/LMAG.2010.2102007.

Prokopenko O V, Bankowski E, Meitzler T, Tiberkevich V S, Slavin A N (2012), "Influence of temperature on the performance of a spin-torque microwave detector," *IEEE Trans. Magn.*, vol. 48, pp. 3807–3810, doi: 10.1109/TMAG.2012.2197853.

Raj A M E, Jayachandran M, Sanjeeviraja C (2010), "Fabrication techniques and material properties of dielectric MgO thin films—A status review," *CIRP J. Manuf. Sci. Technol.*, vol. 2, pp. 92–113, doi: 10.1016/j.cirpj.2010.02.003.

Shang C H, Nowak J, Jansen R, Moodera J S (1998), "Temperature dependence of magnetoresistance and surface magnetization in ferromagnetic tunnel junctions," *Phys. Rev. B*, vol. 58, pp. 2917–2920, doi: 10.1103/PhysRevB.58.R2917.

Sinova J, Valenzuela S O, Wunderlich J, Back C H, Jungwirth T (2015), "Spin Hall effects," *Rev. Mod. Phys.*, vol. 87, pp. 1213–1259, doi: 10.1103/RevModPhys.87.1213.

Sirtori C (2002), "Applied physics: Bridge for the terahertz gap," *Nature*, vol. 417, pp. 132–133, doi: 10.1038/417132b.

Slavin A, Tiberkevich V (2009), "Nonlinear auto-oscillator theory of microwave generation by spin-polarized current," *IEEE Trans. Magn.*, vol. 45, pp. 1875–1918, doi: 10.1109/TMAG.2008.2009935.

Sulymenko O R, Prokopenko O V, Tiberkevich V S, Slavin A N, Ivanov B A, Khymyn R S (2017), "Terahertz-frequency spin Hall auto-oscillator based on a canted antiferromagnet," *Phys. Rev. Appl.*, vol. 8, 064007, doi: 10.1103/PhysRevApplied.8.064007.

Tonouchi M (2007), "Cutting-edge terahertz technology," *Nature Photon.*, vol. 1, pp. 97–105, doi: 10.1038/nphoton.2007.3.

Wadley P, Howells B, Železný J, Andrews C, Hills V, Campion R P, Novák V, Olejník K, Maccherozzi F, Dhesi S S, Martin S Y, Wagner T, Wunderlich J, Freimuth F, Mokrousov Y, Kuneš J, Chauhan J S, Grzybowski M J, Rushforth A W, Edmonds K W, Gallagher B L, Jungwirth T (2016), "Electrical switching of an antiferromagnet," *Science*, vol. 351, pp. 587–590, doi: 10.1126/science.aab1031.

Yuasa S, Djayaprawira D D (2007), "Giant tunnel magnetoresistance in magnetic tunnel junctions with a crystalline MgO(0 0 1) barrier," *J. Phys. D: Appl. Phys.*, vol. 40, R337, doi: 10.1088/0022-3727/40/21/R01.